

# Direct search for features in the primordial bispectrum

Stephen Appleby<sup>a,b,\*</sup>, Jinn-Ouk Gong<sup>b,c,†</sup>, Dhiraaj Kumar Hazra<sup>b,d,‡</sup>, Arman Shafieloo<sup>e,f,§</sup>, and Spyros Sypsas<sup>b,g,¶</sup>

<sup>a</sup>*School of Physics, Korea Institute for Advance Study, Seoul 02455, Korea*

<sup>b</sup>*Asia Pacific Center for Theoretical Physics, Pohang 37673, Korea*

<sup>c</sup>*Department of Physics, Postech, Pohang 37673, Korea*

<sup>d</sup>*AstroParticule et Cosmologie & Paris Centre for Cosmological Physics, Université Paris Diderot, Paris 75205, France*

<sup>e</sup>*Korea Astronomy and Space Science Institute, Daejeon 34055, Korea*

<sup>f</sup>*University of Science and Technology, Daejeon 34113, Korea and*

<sup>g</sup>*Departamento de Física, Universidad de Chile, Santiago 837.0415, Chile*

We study features in the bispectrum of the primordial curvature perturbation correlated with the reconstructed primordial power spectrum from the observed cosmic microwave background temperature data. We first show how the bispectrum can be completely specified in terms of the power spectrum and its first two derivatives, valid for any configuration of interest. Then using a model-independent reconstruction of the primordial power spectrum from the Planck angular power spectrum of temperature anisotropies, we compute the bispectrum in different triangular configurations. We find that in the squeezed limit at  $k \sim 0.1 \text{ Mpc}^{-1}$  and  $k \sim 0.013 \text{ Mpc}^{-1}$  there are marginal  $2\sigma$  deviations from the standard featureless bispectrum, which meanwhile is consistent with the reconstructed bispectrum in the equilateral configuration.

## INTRODUCTION

Recent observational progress on the temperature anisotropies of the cosmic microwave background (CMB) has made primordial inflation [1] the most promising candidate to describe the early universe. Being an effective description at a relatively low energy embedded in an ultraviolet complete theory, it is natural to expect that the inflationary Lagrangian contains substructure which prevents otherwise smooth evolution of the universe during the entire inflation epoch [2]. The resulting features in the primordial correlation functions arising from such substructure imply enhanced interactions, giving rise to a unique observational window to study the unknown physics of the parent theory.

Over the previous decade it has been shown that the primordial power spectrum reconstructed from the observed CMB data allows for the existence of features with roughly 5% modulations in the amplitude [3–5]. Although there is no high confidence detection beyond the smooth power-law form of the primordial power spectrum, the search for features remains tantalizing due to their potential ability to rule out a large class of inflationary scenarios. Furthermore, the existence of features in the primordial power spectrum in turn implies features also in higher order correlation functions. This suggests a compelling way to look for features in the bispectrum by using its correlation with the primordial power spectrum.

In this article, using the primordial power spectrum reconstructed directly from the Planck temperature data [5], we search for scales and triangular configurations at which we would expect non-trivial signals in the bispectrum. The method described in this work, being both fast and accurate, provides an ideal platform to search for correlated features in the primordial bispectrum [6].

## BISPECTRUM IN TERMS OF POWER SPECTRUM

The explicit correlation between the power spectrum of the curvature perturbation  $\mathcal{R}$  and its bispectrum was first elucidated in [7], where the features in the power spectrum are sourced by a non-trivial speed of sound  $c_s$ . This is motivated from an effective single field description of inflation when heavy degrees of freedom are systematically integrated out, which results in non-trivial  $c_s$  for  $\mathcal{R}$  [8]. Given that  $|1 - c_s^{-2}| \ll 1$ , we can explicitly find the leading contributions to the bispectrum  $B_{\mathcal{R}}$  due to a non-trivial  $c_s$  [7]. Moreover, it was noted in [9] that the correlation between correlation functions can be further extended in the context of the generalized slow-roll formalism (GSR) [10] from the relation [11]

$$\log\left(\frac{1}{f^2}\right) = \int_0^\infty \frac{dk}{k} m(-k\tau) \log \mathcal{P}_{\mathcal{R}}(k), \quad (1)$$

where  $f = f(\log \tau) \equiv -2\pi\tau z$ , with  $z^2 \equiv 2a^2\epsilon m_{\text{Pl}}^2/c_s$ ,  $\epsilon \equiv -\dot{H}/H^2$  and  $d\tau \equiv c_s dt/a$ , is the GSR fundamental function and  $m(x) \equiv 2[x^{-2} - x^{-1}\cos(2x) - \sin(2x)]/\pi$ . Then, the “source” of the power spectrum  $(f'' - 3f')/f$  with  $f' \equiv df/d\log \tau$  can be written in terms of  $\mathcal{P}_{\mathcal{R}}$  and its first two derivatives, i.e.  $n_{\mathcal{R}}$  and  $\alpha_{\mathcal{R}}$ .

On totally general grounds, the bispectrum is specified by additional information on the source of the bispectrum  $g_B$  [12], which is obtained from the cubic order action [13]. In the effective field theory point of view [14], the action at each order is specified by a set of mass scales  $M_n^4$ , so that at quadratic order  $M_2^4$  determines  $c_s$ , while at cubic order  $M_3^4$  is to be additionally specified, in principle, as an independent coupling. This is materialized as the bispectrum source  $g_B$ , which is not generically written in terms of the power spectrum source and hence the power spectrum  $\mathcal{P}_{\mathcal{R}}$  and its derivatives. Nevertheless,  $g_B$

can be explicitly connected to  $\mathcal{P}_{\mathcal{R}}$  if we focus our attention on the case in which the most important source of features is specified. An example is given in [7] – a varying  $c_s$  gives rise to the bispectrum source  $g_B$  that has the same origin as the power spectrum source, so we can specify the correlation. The same formula can be derived using the GSR approximation [9].

Another typical and important case is when the inflaton potential  $V(\phi)$  exhibits sudden changes, such as kinks and steps [15–17]. In that case, with  $c_s = 1$ , the dominant source of the features is the variation of  $\epsilon$ , i.e.  $\eta \equiv \dot{\epsilon}/(H\epsilon)$  provided that inflation is not disturbed even with a violent variation of  $\epsilon$  because  $\epsilon \ll 1$  at all times. In this case, GSR is a powerful tool to provide analytic results for the power spectrum [18] as well as the bispectrum [12], which would otherwise require time intensive numerical calculation [5, 19, 20]. The usual cubic action [13] is, however, not appropriate because a term with  $\eta$  is contained in the field redefinition, which we

should later restore by hand. It is thus desirable to use an alternative form of the cubic action where  $\eta$  is explicit outside the field redefinition terms. This form is presented in [21], and collecting only terms with  $\eta$ , we have

$$S_3 \supset \int d^4x a^3 \epsilon m_{\text{Pl}}^2 \left[ -\eta \dot{\mathcal{R}}^2 \mathcal{R} + \frac{\eta}{a^2} \mathcal{R} (\nabla \mathcal{R})^2 \right]. \quad (2)$$

To compute the bispectrum it is convenient, since  $\epsilon \ll 1$ , to consider a perfect de Sitter background where  $\tau = -1/(aH)$ . Then  $\eta$  can be written to leading order in GSR as

$$\eta = - \int_0^\infty \frac{dk}{k} m(-k\tau) \frac{d \log \mathcal{P}_{\mathcal{R}}}{d \log k}. \quad (3)$$

Plugging this expression into (2) with the fluctuations given by the de Sitter mode functions, we derive an alternative form to [7] connecting the bispectrum with the power spectrum and its first two derivatives:

$$B_{\mathcal{R}}(k_1, k_2, k_3) = \frac{(2\pi)^4 \mathcal{P}_{\mathcal{R}}^2}{(k_1 k_2 k_3)^3} \left\{ \int_{K/2}^\infty dk (n_{\mathcal{R}} - 1) \frac{\Delta^2}{k^2} + \left[ (k_1^2 + k_2^2 + k_3^2) \frac{k_1 k_2 + k_2 k_3 + k_3 k_1}{16k} + \frac{(k_1 k_2)^2 + (k_2 k_3)^2 + (k_3 k_1)^2}{8k} - \frac{k_1 k_2 k_3}{8} \right] (1 - n_{\mathcal{R}}) + \frac{k_1 k_2 k_3}{8} \alpha_{\mathcal{R}} \right\}, \quad (4)$$

where  $\mathcal{P}_{\mathcal{R}} = H^2 / (8\pi^2 \epsilon m_{\text{Pl}}^2)$  is the featureless flat power spectrum and the right hand side is evaluated at  $k = (k_1 + k_2 + k_3)/2 \equiv K/2$ . Here,  $\Delta^2 = K(K - 2k_1)(K - 2k_2)(K - 2k_3)/16$  is the area squared of the triangle with three sides  $k_1$ ,  $k_2$  and  $k_3$ . Furthermore, with the  $f_{\text{NL}}$  ansatz [22] in mind, we may define a dimensionless shape function

$$f_{\text{NL}}(k_1, k_2, k_3) \equiv \frac{10}{3} \frac{k_1 k_2 k_3}{k_1^3 + k_2^3 + k_3^3} \frac{(k_1 k_2 k_3)^2 B_{\mathcal{R}}}{(2\pi)^4 \mathcal{P}_{\mathcal{R}}^2}. \quad (5)$$

This can be evaluated in any configuration of interest. In particular, we can reproduce the standard consistency relation in the squeezed limit, say,  $k_3 \ll k_1 \approx k_2$ ,

$$f_{\text{NL}} = \frac{5}{12} (1 - n_{\mathcal{R}}), \quad (6)$$

for (4). The same result can be obtained for the case of a non-trivial speed of sound. Note that (4) is in agreement with the result of [23], where using a different method this formula was derived with the  $\Delta^2$  and  $k_1 k_2 k_3 (1 - n_{\mathcal{R}})/8$  terms missing on the grounds that they are subleading and do not contribute in the squeezed limit.

Before applying our formula (4) to actual data, we have tested the veracity of GSR using a step potential [17, 20]

$$V(\phi) = \frac{1}{2} m^2 \phi^2 \left[ 1 + \alpha \tanh \left( \frac{\phi - \phi_0}{\Delta \phi} \right) \right]. \quad (7)$$

To this end, we numerically calculated the bispectrum using BINGO [19] and compared it with the output of (4). The results are shown in Figure 1, from which we observe excellent agreement, for parameters of the potential such that  $\epsilon \ll 1$  and  $\eta \lesssim 1$ . Thus using GSR, if  $\mathcal{P}_{\mathcal{R}}$  can be estimated independently of any specific inflationary model, then one can make general statements regarding the location and magnitude of any potentially observable features in the bispectrum. However, for sharper departures from slow-roll, where one expects slow-roll parameters to be greater than unity, analytic approximation cannot be trusted and in that case numerical computations (such as using BINGO) can provide the accurate results without approximation.

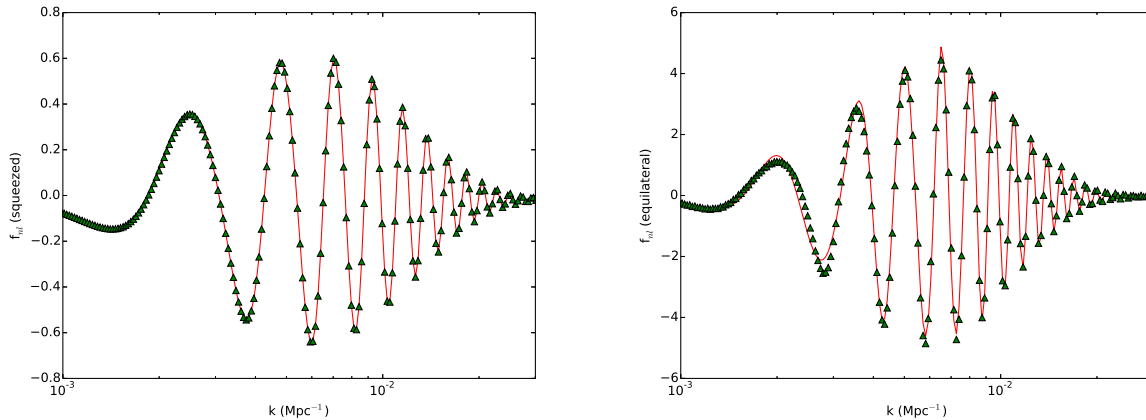


FIG. 1. (Left panel) The  $f_{\text{NL}}$  parameter (5) in the squeezed limit for the inflationary model (7). The solid line indicates the  $f_{\text{NL}}$  calculated by full numerical evaluation of the bispectrum using BINGO, and the triangles correspond to the GSR calculation (5). We observe close agreement at all scales of interest. (Right panel) As in the left panel, but in the equilateral limit. The accuracy of the GSR result is slightly reduced here, however the position and amplitude of the oscillatory structure is successfully captured.

## BISPECTRUM RECONSTRUCTION FROM POWER SPECTRUM

Reconstruction of the primordial power spectrum using the CMB temperature data has been the subject of considerable research over the past decade. Here we adopt the model-independent, non-parametric modified Richardson-Lucy algorithm [4, 5], which relates  $\mathcal{P}_{\mathcal{R}}$  in  $k$ -space to the CMB temperature power spectrum  $\mathcal{C}_{\ell}$  using a convolution of the form

$$\mathcal{C}_{\ell} = \sum_i G_{\ell k_i} \mathcal{P}_{k_i}, \quad (8)$$

where  $G_{\ell k_i}$  is the so-called radiative transport kernel that contains information regarding the background cosmological model and  $i$  denotes the discrete  $k$ -space binning index.  $\mathcal{C}_{\ell}$  is obtained using the 2013 release of Planck temperature data [24], in which we use four frequency channels covering a multipole range  $2 \leq \ell \leq 2500$ . The removal of foregrounds and lensing and the iterative procedure by which (8) is inverted to obtain  $\mathcal{P}_{\mathcal{R}}(k)$  along with all details pertaining to the reconstruction method can be found in [5].

The recovered  $\mathcal{P}_{\mathcal{R}}(k)$  possesses both inflationary features and noise, which is unavoidable. Indeed one cannot make a clear distinction between the two when using a model-independent reconstruction. However, the important point for our purposes is that the shape of the resulting  $\mathcal{P}_{\mathcal{R}}(k)$  is independent of any specific inflationary model, and the location of any significant deviations from a featureless power spectrum can direct our search for corresponding features in the bispectrum.

We generate  $N_{\text{real}} = 1000$  Gaussian realizations of  $\mathcal{C}_{\ell}$ . They are obtained by taking the existing data points

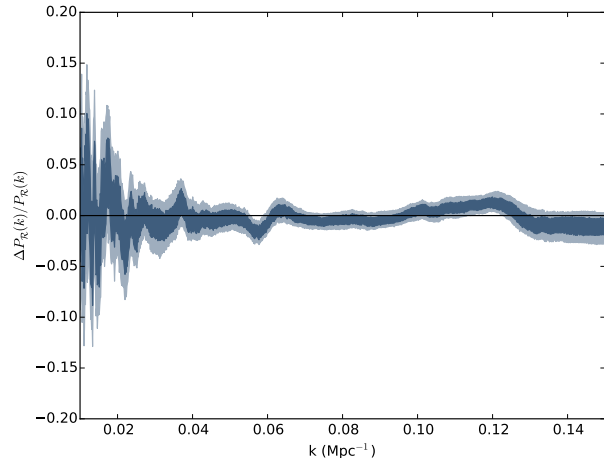


FIG. 2. A model-independent reconstruction of the power spectra according to the procedure outlined in the text. Here we plot the fractional deviation with respect to the best fit power-law model. The dark (light) shaded contours contain 68% (95%) of the  $N_{\text{real}} = 1000$   $\mathcal{P}_{\mathcal{R}}(k)$  curves, that have been reconstructed from  $N_{\text{real}} = 1000$  realizations of the Planck temperature data. The solid line at 0 indicates no deviation from power-law model. There are evidences of features at  $k \sim 0.06 \text{ Mpc}^{-1}$  and  $k \sim 0.12 \text{ Mpc}^{-1}$ .

and adding Gaussian random fluctuations, with variance equal to the diagonal component of the full error covariance matrix. Each  $\mathcal{C}_{\ell}$  is then passed through the iterative procedure outlined in [5] to obtain a corresponding realization of  $\mathcal{P}_{\mathcal{R}}(k)$ . Following this they are smoothed with a Gaussian filter, and the resulting  $\mathcal{P}_{\mathcal{R}}(k)$  provides an improved fit compared to the baseline model. The result

of this operation is exhibited in Figure 2. As reported in [5], we find the maximum deviation from a featureless power spectrum lying at  $k \sim 0.06 \text{ Mpc}^{-1}$  (the other feature near  $k \sim 0.13 \text{ Mpc}^{-1}$  was reported to be a systematic error in Planck).

We now take the  $N_{\text{real}} = 1000$  reconstructed  $\mathcal{P}_{\mathcal{R}}$ 's and estimate their bispectra using (4). To do so, we must numerically calculate the first and second derivatives of  $\mathcal{P}_{\mathcal{R}}(k)$ . This is achieved by constructing a Chebyshev spline to approximate a smooth continuous curve using  $i$  points. We use  $N_{\text{Cheb}}$  Chebyshev polynomials, where  $N_{\text{Cheb}}$  is an integer that dictates the smoothness of the splined curve. We choose  $N_{\text{Cheb}}$  such that the curve provides an equal  $\chi^2$  fit to the Planck temperature data as the non-parametric reconstruction. Based on this criteria, we choose a value of  $N_{\text{Cheb}} = 1000$ : a smaller value degrades the fit, resulting in a larger  $\chi^2$  and a curve that fails to capture the important features in the data, whereas a larger value introduces spurious oscillations that amount to capturing the noise in the data.  $N_{\text{Cheb}}$  is not simply a convenience, it must be chosen carefully to ensure that our smooth approximation properly respects the quality of fit of the non-parametric reconstruction to the data.

Differentiating the Chebyshev fit, we calculate the bispectrum and exhibit  $f_{\text{NL}}$  given by (5) projected onto certain configurations in Figure 3. The left (right) panel exhibits the squeezed (equilateral) configuration. In the insets we magnify limited  $k$ -ranges, highlighting typical behaviour that we observe. In the squeezed configuration, there is a mild anomalous behaviour at  $k \sim 0.1 \text{ Mpc}^{-1}$ , however the amplitude of this deviation from a featureless bispectrum is very small. There is a larger amplitude discrepancy at  $k \sim 0.013 \text{ Mpc}^{-1}$ , also shown in the inset.

In the equilateral limit, the shaded region that represents our reconstructions is larger than in the squeezed limit. This is expected as the second derivative of the power spectrum is no longer suppressed for this triangular configuration. Here the bispectrum corresponding to a flat, featureless power spectrum lies within the 95% bounding region for practically all  $k$ . There are some oscillations, however these are likely to represent noise in the fitting procedure. We arrive at this conclusion by varying  $N_{\text{Cheb}}$  over the limited range  $N_{\text{Cheb}} = (800, 1200)$ : all  $N_{\text{Cheb}}$  in this range provide a roughly comparable fit to the data and the oscillations are insensitive to varying  $N_{\text{Cheb}}$ .

Given that we can reconstruct  $f_{\text{NL}}$  for any configuration, we can perform a general search in  $(k_1, k_2, k_3)$  space for regions with significant deviations from the flat  $\mathcal{P}_{\mathcal{R}}$  expectation. We focus on  $k$ -bands which are known to possess a feature in the power spectrum. Specifically, we fix, say,  $k_1 = 0.1 \text{ Mpc}^{-1}$ , and explore the residual two-dimensional  $(k_2, k_3)$  subspace. We are especially interested in any regions in which the featureless expectation value of  $f_{\text{NL}}$  lies outside the 95% bounded re-

gion of the reconstruction. Hence for each point in the  $(k_2, k_3)$  space, we calculate  $f_{\text{NL}}^{\text{fid}}$ ,  $f_{\text{NL}}^{+2\sigma}$  and  $f_{\text{NL}}^{-2\sigma}$ , where  $f_{\text{NL}}^{\text{fid}}$  is the fiducial value of  $f_{\text{NL}}$ , calculated for a featureless power spectrum with  $n_{\mathcal{R}} = 0.96$ , and  $f_{\text{NL}}^{+2\sigma}$ ,  $f_{\text{NL}}^{-2\sigma}$  are the values that bound 95% of the reconstructed  $f_{\text{NL}}$  from above and below. In Figure 4 we exhibit  $f_{\text{NL}}^{+2\sigma} - f_{\text{NL}}^{\text{fid}}$  and  $f_{\text{NL}}^{-2\sigma} - f_{\text{NL}}^{\text{fid}}$ , plotting over the range  $k_2/k_1 = (0.5, 1.0)$  and  $k_3/k_1 = (10^{-3}, 1)$  - this region will capture all configurations of interest.

The stripes correspond to oscillations in  $f_{\text{NL}}$ , which are observed in Figure 3. Of particular interest are regions in which  $f_{\text{NL}}^{+2\sigma} - f_{\text{NL}}^{\text{fid}} < 0$  and  $f_{\text{NL}}^{-2\sigma} - f_{\text{NL}}^{\text{fid}} > 0$ . These are the regions where the featureless  $f_{\text{NL}}$  lies outside the 95% band, indicating a possible feature. They are exhibited as red (blue) contours in the top (bottom) panel of Figure 4. Such behaviour is most clearly observed in the top left corner of the top panel in Figure 4, indicating a deviation from featureless  $\mathcal{P}_{\mathcal{R}}$  that is most pronounced in the squeezed limit. There are a small number of narrow oscillatory bands which deviate from the featureless limit, however this is probably the same manifestation of noise as found in the equilateral limit.

## CONCLUSION

In this article we search for features in the bispectrum using the primordial power spectrum reconstructed from the angular power spectrum data of CMB temperature anisotropies. This is an important first step in extracting CMB three-point correlations directly from CMB two-point correlations of temperature fluctuations. The method presented is a novel approach that allows a fast and reliable joint analysis of the CMB two- and three-point data. A model-independent reconstruction of the power spectrum can highlight the presence of primordial features that we would expect to see in the bispectrum data, and avoid model comparison with the data using a full Markov Chain Monte Carlo analysis.

Using our method, we find that in the squeezed configuration and in the vicinity  $k \sim 0.013 \text{ Mpc}^{-1}$  and  $k \sim 0.1 \text{ Mpc}^{-1}$  there are potential features with marginal  $2\sigma$  confidence. In the equilateral configuration, the power spectrum reconstructions do not strongly constrain the form of the bispectrum - a featureless bispectrum is consistent but we cannot rule out the possibility of large features being present.

Given the large uncertainty, it is important to confront these findings with CMB three-point temperature correlations directly. A joint constraint on inflationary features using the two- and three-point correlations of temperature and polarization anisotropies is the best possible approach to find or alternatively rule out features with high confidence.

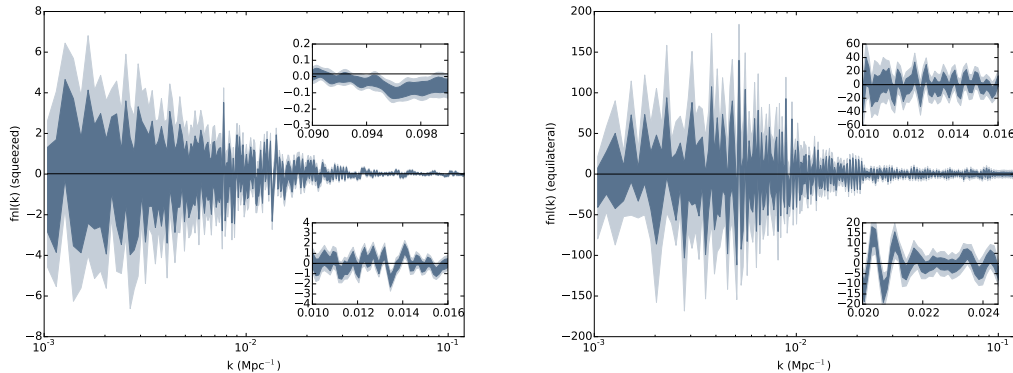


FIG. 3.  $f_{\text{NL}}$  in the (left) squeezed and (right) equilateral limit. The dark (light) band encloses 68% (95%) of the reconstructed  $\mathcal{P}_{\mathcal{R}}$ . We have used  $N_{\text{Cheb}} = 1000$  to fit a smooth curve to the reconstructed power spectrum, which is then used to derive  $f_{\text{NL}}$ . The plot covers the entire range considered in this work,  $k = (10^{-3}, 0.12) \text{ Mpc}^{-1}$ . The inset plots exhibit certain  $k$ -bands of interest. In the squeezed limit we observe some regions in which the bispectrum deviates from its featureless limit, meanwhile we observe no deviation in the equilateral limit. The inset plots in the right panel exhibit typical oscillations around zero which corresponds to noise.

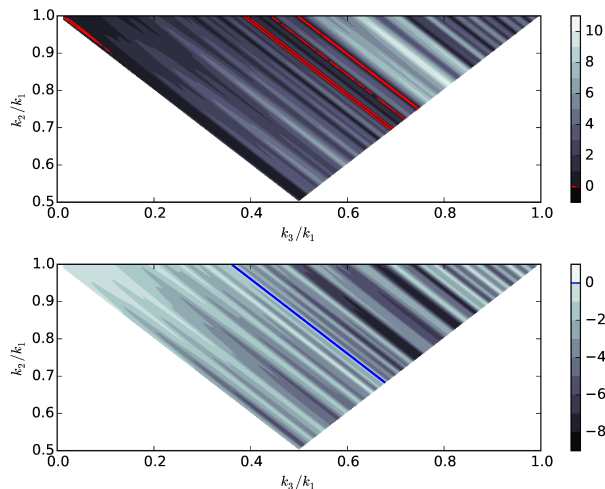


FIG. 4. Heat maps of  $f_{\text{NL}}^{+2\sigma} - f_{\text{NL}}^{\text{fid}}$  (top) and  $f_{\text{NL}}^{-2\sigma} - f_{\text{NL}}^{\text{fid}}$  (bottom) as a function of  $k_3/k_1$  and  $k_2/k_1$ , where we have fixed  $k_1 = 0.1 \text{ Mpc}^{-1}$ . Regions of interest are  $f_{\text{NL}}^{+2\sigma} - f_{\text{NL}}^{\text{fid}} < 0$  and  $f_{\text{NL}}^{-2\sigma} - f_{\text{NL}}^{\text{fid}} > 0$ , indicating areas where the featureless expectation value lies outside the 95% contours. Such regions are exhibited as red (blue) contours in the top (bottom) panel. We observe a small region in the top left corner of the top panel in which  $f_{\text{NL}}^{+2\sigma} - f_{\text{NL}}^{\text{fid}} < 0$ . This is the same deviation as observed in Figure 1. The magnitude of  $f_{\text{NL}}$  is small in this triangular configuration.

## ACKNOWLEDGEMENTS

We thank Jan Hamann, Gonzalo Palma and Paul Shellard for helpful discussions. SA, JG, DKH and SS acknowledge support from the Korea Ministry of Education, Science and Technology, Gyeongsangbuk-Do and

Pohang City for Independent Junior Research Groups at the Asia Pacific Center for Theoretical Physics. JG is also supported in part by a Starting Grant through the Basic Science Research Program of the National Research Foundation of Korea (2013R1A1A1006701) and by TJ Park Science Fellowship of POSCO TJ Park Foundation. DHK acknowledges Laboratoire APC-PCCP, Université Paris Diderot and Sorbonne Paris Cité (DXCACHEXGS) and also the financial support of the UnivEarthS Labex program at Sorbonne Paris Cité (ANR-10-LABX-0023 and ANR-11-IDEX-0005-02). AS would like to acknowledge the support of the National Research Foundation of Korea (NRF-2013R1A1A2013795). SS is supported by the Fondecyt 2016 Post-doctoral Grant 3160299.

\* [stephen@kias.re.kr](mailto:stephen@kias.re.kr)

† [jinn-ouk.gong@apctp.org](mailto:jinn-ouk.gong@apctp.org)

‡ [dhiraj.kumar.hazra@apc.univ-paris7.fr](mailto:dhiraj.kumar.hazra@apc.univ-paris7.fr)

§ [shafieloo@kasi.re.kr](mailto:shafieloo@kasi.re.kr)

¶ [s.sypsas@gmail.com](mailto:s.sypsas@gmail.com)

- [1] A. H. Guth, Phys. Rev. D **23**, 347 (1981) ; A. D. Linde, Phys. Lett. B **108**, 389 (1982) ; A. Albrecht and P. J. Steinhardt, Phys. Rev. Lett. **48**, 1220 (1982).
- [2] See e.g. D. Baumann and L. McAllister, arXiv:1404.2601 [hep-th].
- [3] S. L. Bridle, A. M. Lewis, J. Weller and G. Efstathiou, Mon. Not. Roy. Astron. Soc. **342**, L72 (2003) [astro-ph/0302306] ; A. Shafieloo, T. Souradeep, P. Mani-maran, P. K. Panigrahi and R. Rangarajan, Phys. Rev. D **75**, 123502 (2007) [astro-ph/0611352] ; D. K. Hazra, A. Shafieloo and G. F. Smoot, JCAP **1312**, 035 (2013) [arXiv:1310.3038 [astro-ph.CO]] ; P. Hunt and S. Sarkar, arXiv:1510.03338 [astro-ph.CO].

- [4] A. Shafieloo and T. Souradeep, Phys. Rev. D **70**, 043523 (2004) [astro-ph/0312174] ; D. K. Hazra, A. Shafieloo and T. Souradeep, JCAP **1307**, 031 (2013) [arXiv:1303.4143 [astro-ph.CO]].
- [5] D. K. Hazra, A. Shafieloo and T. Souradeep, JCAP **1411**, no. 11, 011 (2014) [arXiv:1406.4827 [astro-ph.CO]].
- [6] For previous studies, see e.g. A. Achcarro, V. Atal, P. Ortiz and J. Torrado, Phys. Rev. D **89**, no. 10, 103006 (2014) [arXiv:1311.2552 [astro-ph.CO]] ; A. Achucarro, V. Atal, B. Hu, P. Ortiz and J. Torrado, Phys. Rev. D **90**, no. 2, 023511 (2014) [arXiv:1404.7522 [astro-ph.CO]] ; J. R. Fergusson, H. F. Gruetjen, E. P. S. Shellard and M. Liguori, Phys. Rev. D **91**, no. 2, 023502 (2015) [arXiv:1410.5114 [astro-ph.CO]].
- [7] A. Achucarro, J. O. Gong, G. A. Palma and S. P. Patil, Phys. Rev. D **87**, no. 12, 121301 (2013) [arXiv:1211.5619 [astro-ph.CO]].
- [8] A. Achucarro, J. O. Gong, S. Hardeman, G. A. Palma and S. P. Patil, Phys. Rev. D **84**, 043502 (2011) [arXiv:1005.3848 [hep-th]] ; A. Achucarro, J. O. Gong, S. Hardeman, G. A. Palma and S. P. Patil, JCAP **1101**, 030 (2011) [arXiv:1010.3693 [hep-ph]] ; A. Achucarro, J. O. Gong, S. Hardeman, G. A. Palma and S. P. Patil, JHEP **1205**, 066 (2012) [arXiv:1201.6342 [hep-th]].
- [9] J. O. Gong, K. Schalm and G. Shiu, Phys. Rev. D **89**, no. 6, 063540 (2014) [arXiv:1401.4402 [astro-ph.CO]].
- [10] E. D. Stewart, Phys. Rev. D **65**, 103508 (2002) [astro-ph/0110322] ; J. Choe, J. -O. Gong and E. D. Stewart, JCAP **0407**, 012 (2004) [hep-ph/0405155].
- [11] M. Joy, E. D. Stewart, J. -O. Gong and H. -C. Lee, JCAP **0504**, 012 (2005) [astro-ph/0501659] ; M. Joy and E. D. Stewart, JCAP **0602**, 005 (2006) [astro-ph/0511476].
- [12] P. Adshead, W. Hu, C. Dvorkin and H. V. Peiris, Phys. Rev. D **84**, 043519 (2011) [arXiv:1102.3435 [astro-ph.CO]] ; P. Adshead, C. Dvorkin, W. Hu and E. A. Lim, Phys. Rev. D **85**, 023531 (2012) [arXiv:1110.3050 [astro-ph.CO]] ; P. Adshead and W. Hu, Phys. Rev. D **85**, 103531 (2012) [arXiv:1203.0012 [astro-ph.CO]].
- [13] J. M. Maldacena, JHEP **0305**, 013 (2003) [astro-ph/0210603] ; D. Seery and J. E. Lidsey, JCAP **0506**, 003 (2005) [astro-ph/0503692] ; X. Chen, M. x. Huang, S. Kachru and G. Shiu, JCAP **0701**, 002 (2007) [hep-th/0605045] ; J. Martin and L. Sriramkumar, JCAP **1201**, 008 (2012) [arXiv:1109.5838 [astro-ph.CO]].
- [14] C. Cheung, P. Creminelli, A. L. Fitzpatrick, J. Kaplan and L. Senatore, JHEP **0803**, 014 (2008) [arXiv:0709.0293 [hep-th]].
- [15] In a recent article [25] a one-parameter formula for the correlation of the bispectrum and the power spectrum has been derived for the case of both a non-trivial sound speed and potential features upon certain assumptions.
- [16] A. A. Starobinsky, JETP Lett. **55**, 489 (1992) [Pisma Zh. Eksp. Teor. Fiz. **55**, 477 (1992)] ;
- [17] J. A. Adams, B. Cresswell and R. Easther, Phys. Rev. D **64**, 123514 (2001) [astro-ph/0102236] ; L. Covi, J. Hamann, A. Melchiorri, A. Slosar and I. Sorbera, Phys. Rev. D **74**, 083509 (2006) doi:10.1103/PhysRevD.74.083509 [astro-ph/0606452] ; D. K. Hazra, M. Aich, R. K. Jain, L. Sriramkumar and T. Souradeep, JCAP **1010**, 008 (2010) [arXiv:1005.2175 [astro-ph.CO]].
- [18] J. O. Gong, JCAP **0507**, 015 (2005) [astro-ph/0504383] ; C. Dvorkin and W. Hu, Phys. Rev. D **81**, 023518 (2010) [arXiv:0910.2237 [astro-ph.CO]] ; W. Hu, Phys. Rev. D **84**, 027303 (2011) [arXiv:1104.4500 [astro-ph.CO]].
- [19] D. K. Hazra, L. Sriramkumar and J. Martin, JCAP **1305**, 026 (2013) [arXiv:1201.0926 [astro-ph.CO]] ; V. Sreenath, D. K. Hazra and L. Sriramkumar, JCAP **1502**, no. 02, 029 (2015) [arXiv:1410.0252 [astro-ph.CO]].
- [20] X. Chen, R. Easther and E. A. Lim, JCAP **0706**, 023 (2007) [astro-ph/0611645] ; X. Chen, R. Easther and E. A. Lim, JCAP **0804**, 010 (2008) [arXiv:0801.3295 [astro-ph]].
- [21] C. Burrage, R. H. Ribeiro and D. Seery, JCAP **1107**, 032 (2011) [arXiv:1103.4126 [astro-ph.CO]].
- [22] E. Komatsu and D. N. Spergel, Phys. Rev. D **63**, 063002 (2001) [astro-ph/0005036].
- [23] G. A. Palma, JCAP **1504**, no. 04, 035 (2015) [arXiv:1412.5615 [hep-th]].
- [24] P. A. R. Ade *et al.* [Planck Collaboration], Astron. Astrophys. **571**, A15 (2014) [arXiv:1303.5075 [astro-ph.CO]].
- [25] S. Mooij, G. A. Palma, G. Panotopoulos and A. Soto, JCAP **1510**, no. 10, 062 (2015) [arXiv:1507.08481 [astro-ph.CO]].